International Journal of GEOMATE, July, 2024 Vol.27, Issue 119, pp.70-77
ISSN: 2186-2982 (P), 2186-2990 (O), Japan, DOI: https://doi.org/10.21660/2024.119.4384
Geotechnique, Construction Materials and Environment

COHESIVE SOIL BEHAVIOR UNDER CYCLIC LOADING IN UNDRAINED CONDITIONS

*Andrzej Głuchowski[1], Raimondas Šadzevičius[2] , Nerijus Varnas[3] and Wojciech Sas[1]

[1] Department of Geotechnics, Warsaw University of Live Sciences - SGGW, Poland; [2] Kaunas University of Applied Engineering Sciences, Lithuania; [3] Department of Water Engineering, Vytautas Magnus University Agriculture Academy

*Corresponding Author, Received: 17 Jan. 2024, Revised: 07 Feb. 2024, Accepted: 07 March 2024

ABSTRACT: In this paper, a study of the cyclic plastic creep phenomenon during cyclic loading was performed. The plastic creep phenomena in the field of soil cyclic loading are defined as a process that occurs under a medium stress state and leads to excessive accumulation of plastic strains. Recent literature shows the existence of plastic creep, which is a part of the shakedown theory for cohesive soils. Nevertheless, when the soil is subjected to a relatively small stress state, the axial plastic strain may occur as a phenomenon called *abation*, where plastic strain increment occurs in a constant decreasing manner. Cyclic triaxial tests were performed to understand the abation. The results indicate a specific phase in soil response, such as pre-failure stages marked by pore pressure increase and subsequent effective stress reduction, indicating a steady state during repeating loading. In this paper, the proposition of a cyclic plastic creep mechanism based on test results is presented. The soil response was divided into three phases based on the pore pressure, stress paths, resilient modulus, and plastic strain change analysis.

Keywords: Abation, Cyclic loading, Plastic creep, Pore pressure Resilient modulus, Shakedown, Triaxial test

1. INTRODUCTION

Cohesive soils subjected to cyclic loading behave differently in comparison to non-cohesive soils. Studies on unbounded granular materials, which are a common subbase material, led to the establishment of a new standard of non-destructive testing. The standard BN-EN 13286:2004 [1], establishes a definition of resilient modulus and shakedown in geotechnical engineering design by EUROCODE 7. However, there is still little knowledge about this parameter and phenomenon. The above-mentioned standard refers only to unbounded coarse materials. The fine-graded soils are omitted, not without a good reason. The studies regarding cohesive soil response to cyclic loading were conducted over many years but only for a low number of cycles ($N < 100$) or for high-stress levels, and recently, the scope of these tests was extended to long-term cyclic loading [2,3].

Studies of the impact of cyclic loading on pore pressure have shown different excess pore water pressure development, which was dependent on the stress state [4–9]. The cyclic loading of normally consolidated cohesive soil samples in undrained conditions causes movement of the effective stress path toward the deviator stress axis, which can be recognized as a consolidation state [10–13]. The preconsolidated soils, opposite to normally consolidated ones, loaded in the same stress state conditions, generate lower excess pore water pressure, which results in the decrease of compressive strength in undrained conditions [14–16].

The stress state conditions under which soil samples were tested show that there exists a certain limit under which cohesive soil will respond differently to cyclic loading [17–22]. This statement is like the proposition of Werkmeister [23] and refers to the shakedown theory. The shakedown in the field of cyclic loading is divided into three categories of the soil response to cyclic loading: *Plastic shakedown*, which can be depicted as a close-up hysteresis loop in stress-strain function. In this case, the deviator stress value is low, and after a few cycles of loading, no additional plastic strains are observed [24]. *Cyclic plastic creep* is a phenomenon observed during constant loading tests. Soil samples loaded by force will accumulate a plastic strain during numerous repetitions. The value of accumulated plastic strains is again dependent on the stress state and rises with the increase of deviator stress [25].

Ratchetting, is a phenomenon that is observed at the high-stress state level. The soil sample will fail due to an increase of excess pore pressure after a few cycles [26]. The term low, medium, or high-stress state in the case of unbound coarse aggregates is not specified. In EUROCODE 7 the classification of the stress state is done by strain – number of cycles curve analysis. The plastic shakedown zone limit for subbase material, in terms of strain, is defined as follows (1) [1]:

$$\boldsymbol{\varepsilon_{p5000} - \varepsilon_{p3000} < 0.4 \cdot 10^{-3}} \quad (1)$$

where ε_{p3000} and ε_{p5000} are plastic strains after 3000 and 5000 cycles.

In past years, most extensive tests were performed for phenomena of ratcheting which is observed in case of high deviatory stress in triaxial tests. Eventual exceptions to the pattern of soil response observed in the *ratcheting* zone were accounted to the *cyclic*

plastic creep [27–31].

Studies performed by Werkmeister [19,32] were devoted to the subject of unbound granular materials. The phenomenon of shakedown was also recognized for cohesive soils [33,34]. Nevertheless, the shakedown limits which divide the possible range of soil responses in case of cohesive soil have not been established yet. The reason for that is the different nature of clay deposits than non-cohesive soils. The adhesion forces between particles, low permeability, and different soil skeleton structure, hind a proper identification of shakedown occurrence [35].

Recently, the scope of the research topic concerning cyclic loading of soil phenomena was turned to soft clay deposits. The studies involve tests in undrained conditions under different stress states. The undrained condition is the most preferable type of triaxial test in case of repeating loading of cohesive soils. The drained cyclic tests are preferable mostly for non-cohesive soils where, for example, compaction phenomena are studied [36]. This type of loading occurs usually in a certain range of frequencies from 0.01 to 2 or 5 Hz [37]. The lower limit value responds to the impact of secondary consolidation phenomena, which can interrupt the test results. The upper limit separates the quasi-static loading from dynamic loading. The quasi-static loading is defined in this case as a repeating loading that does not cause an inertia effect. To reach this goal, not only the frequency must be in a certain range but also the amplitude of loading and therefore, the upper limit is in a wide range [38].

The cyclic loading applied in constant stress conditions leads to cohesive soil reaction in form of plastic strains. The accumulated plastic strains can have various characteristics in terms of intensity. Studies on the form of accumulated irreversible strains performed by Goldscheider and Gudehus [39] for shallow foundations subjected to cyclic loading lead to the distinction of different deformation behavior. The deformation behavior was divided into three categories, a *stepwise failure*, an *abation*, and *shakedown*. The *stepwise failure* is a case where accumulated deformations lead to the failure of construction. The *abation* phenomenon occurs when the rate of deformation accumulation decreases with every cycle but it never vanishes completely [37]. The *shakedown* is a type of plastic deformation accumulation where after a number of cycles, there are no additional plastic deformations and soil response is completely elastic [40]. The aim of this research is to understand cohesive soil's deformation behavior and ratcheting effects under cyclic loading is crucial for geotechnical engineering and road engineering designers.

2. RESEARCH SIGNIFICANCE

This research shows the significance of cyclic plastic creep phenomenon during cyclic loading of cohesive soils. It expands our knowledge of soil behavior under medium stress states and reveals the lesser-known *abation* effect under smaller stress states. By conducting cyclic triaxial tests, the study unveils a *cyclic plastic creep mechanism*, dividing soil response into distinct phases. These findings are crucial for understanding cohesive soil's deformation behavior and ratcheting effects under cyclic loading, contributing to a deeper grasp of soil mechanics in geotechnical engineering.

3. MATERIAL AND METHODS

3.1 Material Properties

The material in this study was a cohesive soil consisting of sand, silt, and clay fraction in the following distribution: 41, 39, and 20%, respectively. By using the EUROCODE 7 soil classification ISO triangle, the cohesive material was recognized as sandy silty clay (sasiCl) [41]. For tested soil, the Atterberg limits were determined. The liquid limit LL was equal to 42.5% and the plasticity limit was equal to 22.5%. The plasticity index IP, therefore, was equal to 20%, and the tested soil was classified as a high plasticity clay CL based on the Casagrande plasticity chart.

Tested three soil samples were prepared by compaction with respect to the Proctor method. In this study preliminary, Proctor's tests results have shown optimal moisture content equal to 12.5%. The maximum dry density was equal to 1.95 $g \cdot cm^{-3}$. The triaxial test soil samples with a diameter equal to 7cm and height equal to 14cm were compacted at optimal moisture content. The energy of compaction was equal to $E_c = 0.59\ J \cdot cm^{-3}$.

3.2 Test Preparation and Test Procedure

All the triaxial tests were conducted in the same manner. After sample installation in the triaxial apparatus, a saturation stage was performed. The saturation process was terminated when Skempton parameter *B* was equal to 0.93. The next stage was an isotropic consolidation, in which the isotropic consolidation stress σ'_3 was equal to 45 kPa. The consolidation phase was terminated when no leakage of pore water from the sample was observed. After these two steps, the main tests started. The cyclic loading test program presents in Table 1.

Table 1. Program of cyclic triaxial tests in this study.

Test	q_{max} [kPa]	q_{min} [kPa]	q_m [kPa]	q_a [kPa]	σ'_3 [kPa]
1.1	43	21	32	11	
1.2	53	21	37	16	45
1.3	65	21	43	22	

where, q_{max} – maximal deviator stress, q_{min} – minimum deviator stress, q_m – deviator stress median, q_a – deviator stress amplitude.

The three stages of cyclic loading were performed in constant stress conditions presented in Table 1. For each step, 10000 cycles were applied at a frequency equal to 1 Hz. During the test, the value of vertical axial strain ε1, deviator stress q, pore pressure u, and cell pressure was measured, calculated, and registered in the raw data file.

4. RESULTS AND DISCUSSION

The repeated loading triaxial test results in Cambridge stress characteristics are presented in Fig. 1.

Presented stress path characteristics for test 1.1 indicates pore pressure increase during the test. The stress path is moving towards the deviator stress *q* axis which means that the effective stress *p'* decreases. The process is most intensive at the beginning of the test and with the following cycles reduces. The red color on this plot indicates the last 100 cycles. The stress path remains in the same shape and the further decrease of effective stress is small in comparison to the first few cycles. Test 1.2. which was conducted by applying greater deviator stress, leads to further development of pore pressure and therefore to the decrease of effective stress. The rate of change was smaller when compares to test 1.1. The stress path in this test is moving towards the deviator stress axis but in a certain phase of the test, it changes its direction. This means an increase in the effective pressure caused by the decrease of the pore pressure value.

Test 1.3 which was conducted in the highest planned stress state has led to soil failure in the first few cycles which can be observed as the effective stress increase. This phenomenon was recognized by the fact that the stress path moves away from the deviator stress axis and is explained further in this article.

Fig. 2 presents an excess pore water pressure versus the number of cycles and vertical axial strain ε_1 for all three tests respectively. The excess pore water pressure in test 1.1 reaches its peak in around 1500 cycles and after decreases. The maximum excess pore water pressure Δu is equal to 32 kPa. During the test axial permanent strain is developing and the most extensive irrecoverable strain increase was observed in the phase during which, the excess pore water pressure grows as well.

This phase which constitutes 15% of time loading caused around 1% of plastic strain and the rest 85% of time loading had led to a further 0.12% of plastic strain development. Therefore, it can be clearly stated that, during the first phase of cyclic loading, soil responds to cyclic loading with plastic strain development, and this is accompanied by rapid pore pressure growth. The beginning of the pore pressure decrease phase indicates excessive plastic strain growth termination.

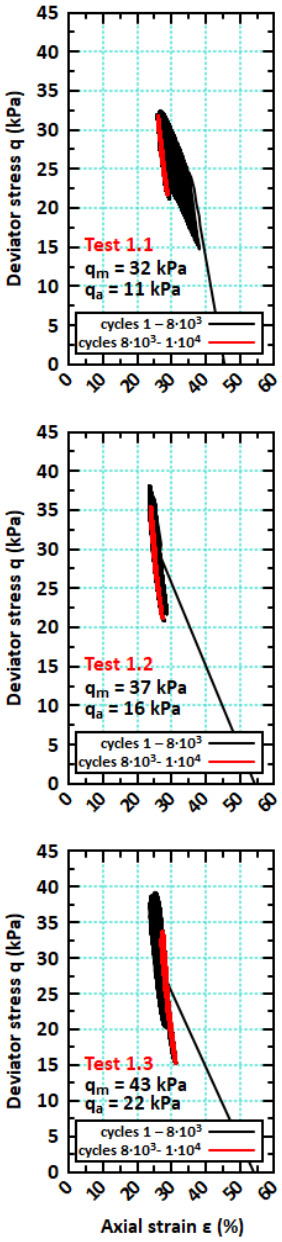

Fig.1 Plot of effective stress and deviator stress repeated loading triaxial test for sandy-silty clay.

This process is characterized by constant pore pressure decrease and plastic strain development at a lower rate than in the previous phase. When the rate of pore pressure decreases to zero, a third phase starts. The excess pore water pressure remains almost at the same level and plastic strains development vanishes almost completely. Soil skeleton reaches optimum configuration and no additional plastic strains in the cycle can be observed.

Nevertheless, after numerous repetitions, some additional strains occur. These strains might be caused by secondary effects which are connected to the *cyclic plastic creep* phenomenon.

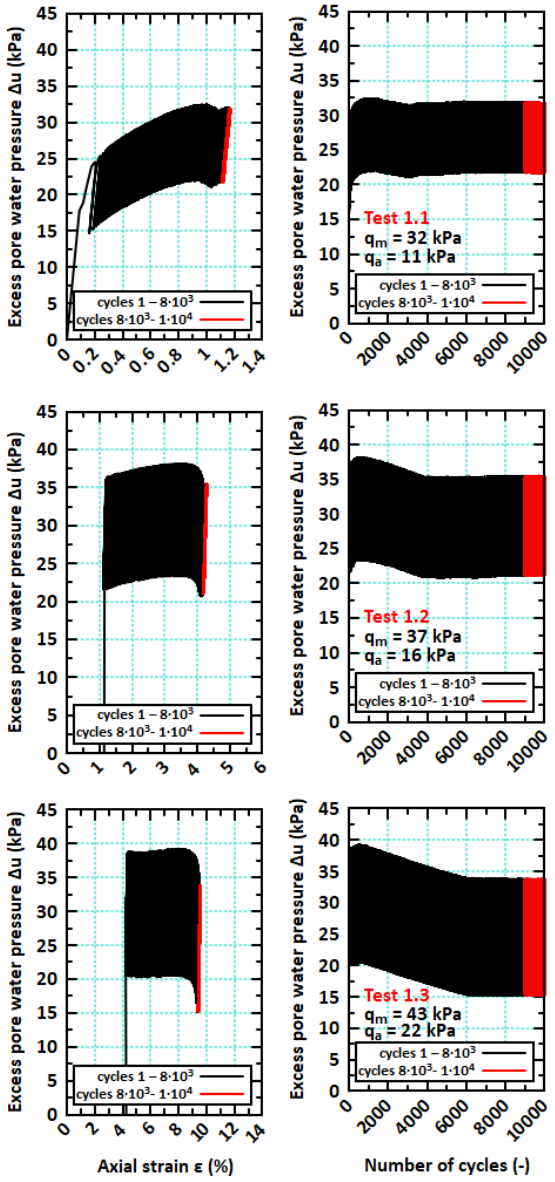

Fig.2 Plot of pore pressure u development during repeated loading triaxial test on sandy silty clay sample.

In the case of tests 1.2 and 1.3, the same pattern can be observed. The first phase occurs with increasing pore water pressure and extensive plastic strains. The greatest difference which can be simply noted is connected to the time of occurrence of the individual phases. The peak pore pressure is reached earlier, and the second phase lasts longer. This phenomenon is connected to a higher maximum deviator stress value. The maximal pore water pressure Δu_{max} increases, as well as the deviator stress value and minimum pore water pressure, decreases simultaneously.

The first phase can be identified as a pre-failure stage where the increase of pore water pressure leads to a reduction of the effective stress and later to a critical state. Nevertheless, the constant stress method prevents continuing the process of loading, and effective stress rises which can be observed in the second step. The process continues until a steady state of stress which is characterized by pore pressure stabilization is not reached. Once, when the steady-state is achieved, the process of deformation due to effective stress p' reduction is completed. The plastic strains which occur during these two stages are dependent on deviator stress value, especially on q_a and q_m values but also on other factors, which were not analyzed in this study and might be important, for example, effective consolidation stress σ'_3, initial void ratio $e_{0,}$ and the frequency.

In Figure 3 stress-strain characteristics for distinct cycles were presented. The characteristics enable the analysis of elastic properties of tested soil. In all three tests, stress-strain characteristics are in the shape of the hysteresis loop. The hysteresis loop occurrence during the test is a representation of the dissipation of energy of loading.

An area of the hysteresis loop represents an amount of energy dissipated during loading. In test 1.1 the first loading cycle caused plastic strain equal to 0.028%. The elastic strain was equal to 0.052% which is 65% of total strains in this cycle. The elastic and plastic strains were calculated based on (2):

$$\varepsilon_T = \varepsilon_{R1} + \varepsilon_{P1} \quad (2)$$

where the ε_{R1} is vertical resilient (elastic) strain and ε_{P1} is vertical plastic strain. The elastic strain value in the first cycle seems to be high, but the soil in this study was compacted which means, that this soil has a high value of the preconsolidation pressure and the radial pressure σ'_3 is equal to 45 kPa. In the 10^{th} cycle, the plastic strain constitutes 0.5%. The plastic strain in further cycles is less than 0.3%. With the number of cycles the slope of the hysteresis loop is increasing which represents the hardening phenomena. With the hardening process, the reduction of the hysteresis loop area is observed.

Another characteristic can be observed in the case of tests 1.2 and 1.3. In these tests the soil responds to cyclic loading in the first cycle and is stiffer than further cycles. Plastic strains are less than 2% of total strains and greater plastic strain can be observed in cycles 10 and 100. Even after a high accumulation of strains in test 1.2 after 10000 cycles, an increase of deviator stress in test 1.3 resulted in a similar response as in test 1.2. The lowest stiffness in both tests was observed in cycle 100. In cycle 1000 the stiffness increased, and the area of the hysteresis loop decreased. This corresponds to the phenomenon observed in the second stage of the pore pressure development mechanism. The shape of the 10000 cycles in tests 1.2 and 1.3 is similar to the shape observed in test 1.1.

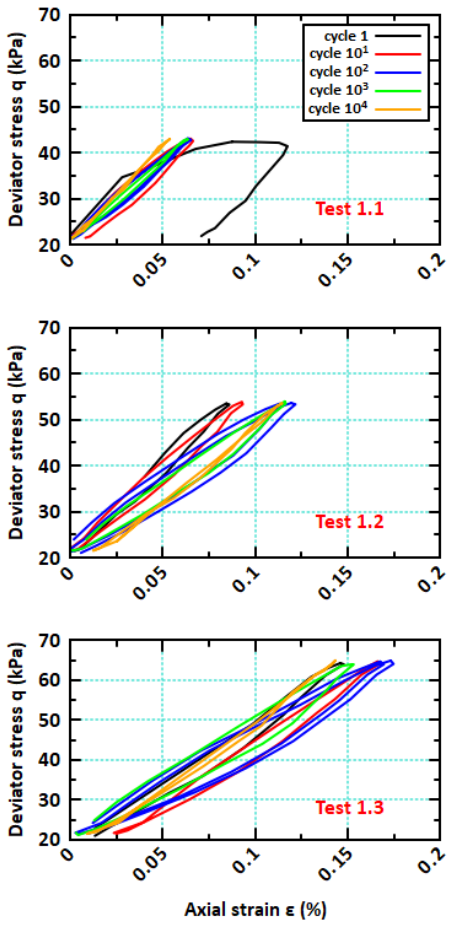

Fig.3 Plot of pore pressure *u* development during repeated loading triaxial test on sandy silty clay sample.

Elastic strains can be represented by the resilient modulus M_r value which is defined as (3):

$$M_r = \frac{q_{max} - q_{min}}{\varepsilon_{R1}} \quad (3)$$

The calculations of resilient modulus value were performed to characterize the change in soil stiffness. Fig. 4 presents the values of resilient modulus characteristics versus the number of cycles.

In all three cases, the resilient modulus was changing in the same pattern. The first cycle is characterized by the high M_r value. Further cycles lead to the decrease of resilient modulus value and the lowest M_r is observed between 200th and 300th cycle. After this point, the resilient modulus starts to increase. Figure 5 presents plastic strain ε_{P1} and maximum excess pore water pressure Δu_{max} versus the number of cycles in a logarithmic scale. The abovementioned threshold number of cycles where the rate of resilient modulus changes, is also a turning point in the case of plastic strains where rapid change of characteristics can be observed[19].

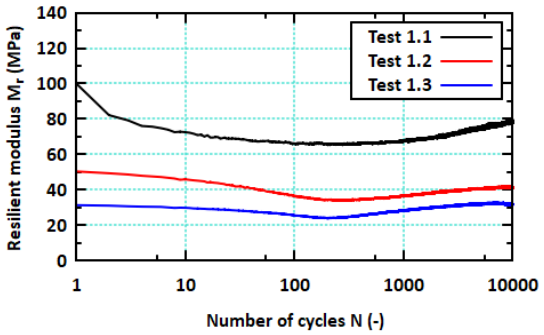

Fig.4 Resilient modulus characteristics during cyclic triaxial test for different values of deviator stress.

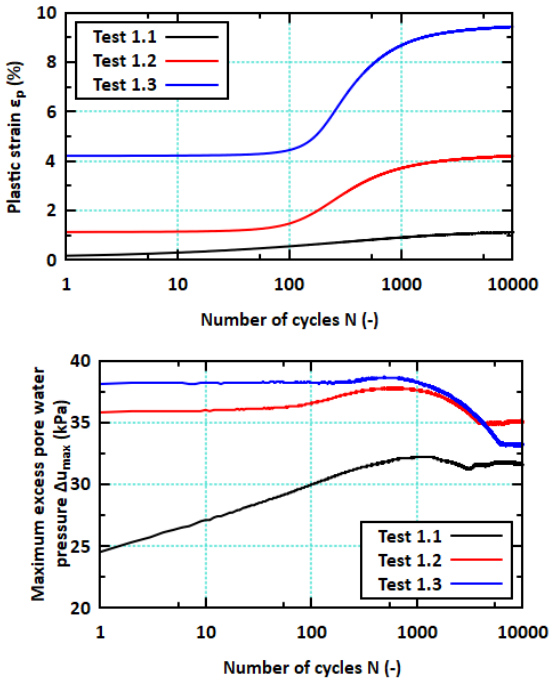

Fig.5 The characteristics of plastic strain development and maximal excess pore water pressure versus the number of cycles for sandy silty clay.

Such behavior is not observed in the case of pore water pressure. This also means that the first phase of cyclic loading is composed of two parts. The first one includes stiffness degradation. When the resilient modulus reaches its lowest value then the hardening process starts and a decrease in plastic strains rate is observed.

In Table 2 results of EUROCODE 7 calculations are presented based on Equation (1). The results show that none of the three tests meet the Werkmeister limit proposition. Based on the definition of shakedown limits, all three tests were in the cyclic plastic creep zone.

The response of compacted sandy silty clay to cyclic loading was analyzed in this study. A mechanism of soil response that is a part of cyclic

plastic creep in shakedown theory was recognized. Test results for cohesive soil loaded by cyclic force have led to plastic creep response based on EUROCODE 7 limit. Nevertheless, the limit was established for non-cohesive soils and direct comparison might be not correct.

Table 2. Results of calculation of soil response to cyclic loading based on EUROCODE 7 shakedown criteria.

Test no.	1.1	1.2	1.3
ε_{P3000} [%]	1.08	4.15	9.37
ε_{P5000} [%]	1.13	4.23	9.46
$\Delta\varepsilon_P$ [%]	0.0407	0.076	0.0995
$\Delta\varepsilon_P$ [-]	0.0004	0.00076	0.00099
EUROCOE 7 limit [-]		0.0004	

ε_{P3000} – accumulated plastic strain at 3000th cycle, ε_{P5000} – accumulated plastic strain at 5000th cycle

5. CONCLUSIONS

Based on three cyclic loading tests conducted in different deviator stress conditions, the reaction of cohesive soil to cyclic loading in undrained conditions, for the cyclic plastic creep zone, was divided into three phases.

1. During the first phase of cyclic loading, soil responds to cyclic loading with plastic strain development and rapid pore pressure growth. This phase was divided into two stages based on resilient modulus change analysis.

a. The first stage is characterized by rapid stiffness drop and moderate plastic strain accumulation. During this stage, pore pressure grows at a constant rate.

b. The second stage is characterized by the lowest value of the stiffness, and which can be observed with the high rate of the plastic strain accumulation. The excess pore water pressure does not follow this pattern and rises at the same rate as in the first stage.

2. The second phase starts when the pore water pressure decrease is observed. The plastic strain rate decreases in each cycle which is similar to the abation phenomena.

3. The third phase begins when the excess pore water pressure remains almost at the same level and plastic strain accumulation is almost not observed. Soil skeleton reaches optimum configuration and no additional plastic strains in one cycle can be observed.

In the performed test, the plastic strains were registered in the third phase. This occurrence can be noted only when multiple cycles are analyzed, and these plastic strains are caused by secondary effects which are connected to the cyclic plastic creep phenomena.

The first phase of cyclic plastic creep behavior was identified as the pre-failure stage caused by the increase of pore water and reduction of the effective stress. Nevertheless, the constant stress method applied in this cyclic triaxial test prevents continuing soil samples from failure and effective stress rises which can be observed as the second step.

The above-presented mechanism shows how cohesive soil reacts to cyclic loading in undrained conditions. The observed cyclic plastic creep response of the soil sample was the same for different stages of applied deviator stress value.

The previous works on the topic on cohesive soil stiffness degradation in undrained conditions shows, that (i) the stiffness degradation and plastic strain accumulation are governed by cyclic stress paths with deviatoric stress variation [42], (ii) .excess pore water pressure accumulated during cyclic loading reduces soil strength, and when the sample is allowed to drain, the soil strength increases [43], (iii) plastic strains development leads to critical shear strain level, called yield shear strain, where softening starts [44]. The presented above summary shows that the literature agrees with the presented here conclusions.

The recommendation is to include *abation* as a possible way of response of cohesive soil in undrained conditions during cyclic loading. The test results indicate that there is rather soft change between soil response rather than one which can be represented by limits in the case of non-cohesive soils.

6. ACKNOWLEDGMENTS

The work reported here was carried out within the Preludium project financed by the National Science Centre, Poland (contract number 2016/23/N/ST10/02185). The authors wish to express their gratitude to the National Science Centre for its financial support.

REFERENCES

1. BS EN 13286-7:2004 Unbound and Hydraulically Bound Mixtures Cyclic Load Triaxial Test for Unbound Mixtures; BS EN 13286-7:2004; Under Review.; 2004; ISBN 978-0-580-43473-0.
2. Zhang, Q.; Cao, Z.; Cai, Y.; Gu, C.; Wang, J. Experimental Investigation into the Cyclic Behaviour of Geogrid Enhanced Base Layer Aggregate through Large-Diameter Triaxial Tests. Transportation Geotechnics 2022, Vol. 37, 100851.
3. Zhu, S.; Chen, R.-P.; Yin, Z.-Y. Elastoplastic Modeling of Cyclic Behavior of Natural Structured Clay with Large Number of Cycles.

Transportation Geotechnics 2021, Vol. 26, 100448.
4. Tang, Y.-Q.; Zhou, J.; Liu, S.; Yang, P.; Wang, J.-X. Test on Cyclic Creep Behavior of Mucky Clay in Shanghai under Step Cyclic Loading. Environ Earth Sci 2011, Vol. 63, pp. 321–327.
5. Vucetic, M.; Dobry, R. Degradation of Marine Clays under Cyclic Loading. J. Geotech. Engrg. 1988, Vol. 114, pp. 133–149.
6. Ansal, A.; İyisan, R.; Yıldırım, H. The Cyclic Behaviour of Soils and Effects of Geotechnical Factors in Microzonation. Soil Dynamics and Earthquake Engineering 2001, Vol. 21, pp. 445–452.
7. Sas, W.; Gabryś, K.; Soból, E.; Szymański, A. Dynamic Characterization of Cohesive Material Based on Wave Velocity Measurements. Applied Sciences 2016, Vol. 6, 49.
8. Arvin, M.R.; Askari, F.; Farzaneh, O. Seismic Behavior of Slopes by Lower Bound Dynamic Shakedown Theory. Computers and Geotechnics 2012, Vol. 39, pp. 107–115.
9. Boulbibane, M.; Weichert, D. Application of Shakedown Theory to Soils with Non Associated Flow Rules. Mechanics Research Communications 1997, Vol. 24, pp. 513–519.
10. Kalinowska, M.; Jastrzębska, M. Behaviour of Cohesive Soil Subjected to Low-Frequency Cyclic Loading in Strain-Controlled Tests. Studia Geotechnica et Mechanica 2015, Vol. 36, pp. 21–35.
11. Li, H.X.; Yu, H.S. A Nonlinear Programming Approach to Kinematic Shakedown Analysis of Frictional Materials. International Journal of Solids and Structures 2006, Vol. 43, pp. 6594–6614.
12. Cai, Y.; Gu, C.; Wang, J.; Juang, C.H.; Xu, C.; Hu, X. One-Way Cyclic Triaxial Behavior of Saturated Clay: Comparison between Constant and Variable Confining Pressure. J. Geotech. Geoenviron. Eng. 2013, Vol. 139, pp. 797–809.
13. Ni, J.; Indraratna, B.; Geng, X.-Y.; Carter, J.P.; Rujikiatkamjorn, C. Radial Consolidation of Soft Soil under Cyclic Loads. Computers and Geotechnics 2013, Vol. 50, pp. 1–5.
14. Guo, L.; Wang, J.; Cai, Y.; Liu, H.; Gao, Y.; Sun, H. Undrained Deformation Behavior of Saturated Soft Clay under Long-Term Cyclic Loading. Soil Dynamics and Earthquake Engineering 2013, Vol. 50, pp. 28–37.
15. Yasuhara, K.; Hirao, K.; Hyde, A.F.L. Effects of Cyclic Loading on Undrained Strength and Compressibility of Clay. Soils and Foundations 1992, Vol. 32, pp. 100–116.
16. Yasuhara, K.; Murakami, S.; Song, B.-W.; Yokokawa, S.; Hyde, A.F.L. Postcyclic Degradation of Strength and Stiffness for Low Plasticity Silt. J. Geotech. Geoenviron. Eng. 2003, Vol. 129, pp. 756–769.
17. Werkmeister, S.; Dawson, A.R.; Wellner, F. Permanent Deformation Behavior of Granular Materials and the Shakedown Concept. Transportation Research Record 2001, Vol. 1757, pp. 75–81.
18. Boulbibane, M.; Ponter, A.R.S. The Linear Matching Method for the Shakedown Analysis of Geotechnical Problems. Int. J. Numer. Anal. Meth. Geomech. 2006, Vol. 30, pp. 157–179.
19. Werkmeister, S. Shakedown Analysis of Unbound Granular Materials Using Accelerated Pavement Test Results from New Zealand's CAPTIF Facility. In Proceedings of the Pavement Mechanics and Performance; American Society of Civil Engineers: Shanghai, China, May 11 2006; pp. 220–228.
20. Hu, C.; Liu, H.; Huang, W. Anisotropic Bounding-Surface Plasticity Model for the Cyclic Shakedown and Degradation of Saturated Clay. Computers and Geotechnics 2012, Vol. 44, pp. 34–47.
21. Pande, G.N. Shakedown of Foundations Subjected to Cyclic Loads.; John Wiley & Sons New York; Vol. 1, pp. 469–489.
22. Ponter, A.R.S.; Hearle, A.D.; Johnson, K.L. Application of the Kinematical Shakedown Theorem to Rolling and Sliding Point Contacts. Journal of the Mechanics and Physics of Solids 1985, Vol. 33, pp. 339–362.
23. Werkmeister, S.; Dawson, A.R.; Wellner, F. Permanent Deformation Behaviour of Granular Materials. Road Materials and Pavement Design 2005, Vol. 6, pp. 31–51.
24. Cui, K.; Qing, Y.; Li, Q.; Zhang, D.; Li, P.; Liu, J. Plastic Shakedown Limit of Compacted Clay: Experiments and Predicted Model. Engineering Geology 2023, Vol. 320, 107057.
25. Nair, L.; Rujikiakamjorn, C.; Indraratna, B. The Importance of Principal Stress Rotation in Transportation Geotechnics and Associated Constitutive Models.; Kochi, 17/12 2022; Vol. TH-12-038, pp. 1–14.
26. Chen, L.; Ghorbani, J.; Kodikara, J. Modelling of Shakedown, Ratcheting and Liquefaction of Saturated Granular Soils Using Kinematic Hardening with Memory Surface. Computers and Geotechnics 2024, Vol. 165, 105830.
27. Sas, W.; Głuchowski, A.; Gabryś, K.; Soból, E.; Szymański, A. Deformation Behavior of Recycled Concrete Aggregate during Cyclic and Dynamic Loading Laboratory Tests. Materials 2016, Vol. 9, 780.
28. Sas, W.; Głuchowski, A.; Gabryś, K.; Soból, E.; Szymański, A. Resilient Modulus Characterization of Compacted Cohesive Subgrade Soil. Applied Sciences 2017, Vol. 7, 370.
29. Sas, W.; Głuchowski, A.; Gabryś, K.; Soból, E.; Szymański, A. Studies on Cyclic and Dynamic

Loading on Cohesive Soil in Road Engineering. In Proceedings of the Proceedings of 13th Baltic Sea Geotechnical Conference; Vilnius Gediminas Technical University: Vilnius Gediminas Technical University, September 24 2016; pp. 85–92.
30. Wu, T.; Han, J.; Cai, Y.; Guo, L.; Wang, J. Relationship between Monotonic and Cyclic Behavior of Saturated Soft Clay in Undrained Triaxial Compression Tests. Can. Geotech. J. 2021, Vol. 58, pp. 1812–1824.
31. Liu, Z.; Xue, J. The Deformation Characteristics of a Kaolin Clay under Intermittent Cyclic Loadings. Soil Dynamics and Earthquake Engineering 2022, Vol. 153, 107112.
32. Yu, H.S.; Khong, C.D.; Wang, J.; Zhang, G. Experimental Evaluation and Extension of a Simple Critical State Model for Sand. Granular Matter 2005, Vol. 7, pp. 213–225.
33. Tao, M.; Mohammad, L.N.; Nazzal, M.D.; Zhang, Z.; Wu, Z. Application of Shakedown Theory in Characterizing Traditional and Recycled Pavement Base Materials. J. Transp. Eng. 2010, Vol. 136, pp. 214–222.
34. Yu, H.S.; Hossain, M.Z. Lower Bound Shakedown Analysis of Layered Pavements Using Discontinuous Stress Fields. Computer Methods in Applied Mechanics and Engineering 1998, Vol. 167, pp. 209–222.
35. Głuchowski, A.; Sas, W. Impact of Cyclic Loading on Shakedown in Cohesive Soils—Simple Hysteresis Loop Model. Applied Sciences 2020, Vol. 10, 2029.
36. Dob, H.; Messast, S.; Mendjel, A.; Boulon, M.; Flavigny, E. Behavior of Sand After a High Number of Cycles Application to Shallow Foundation. Int J Civ Eng 2016, Vol. 14, pp. 459–465.
37. Wichtmann, T.; Niemunis, A.; Triantafyllidis, Th. Strain Accumulation in Sand Due to Cyclic Loading: Drained Triaxial Tests. Soil Dynamics and Earthquake Engineering 2005, Vol. 25, pp. 967–979.
38. Guzev, M.; Kozhevnikov, E.; Turbakov, M.; Riabokon, E.; Poplygin, V. Experimental Studies of the Influence of Dynamic Loading on the Elastic Properties of Sandstone. Energies 2020, Vol. 13, 6195.
39. Goldscheider, M.; Gudehus, G. Einige bodenmechanische Probleme bei Kusten und Offshore-Bauwerken.; DGEG: Nurnberg, Germany, 1976; Vol. 1, pp. 507–522.
40. Wang, K.; Chen, Z.; Wang, Z.; Chen, Q.; Ma, D. Critical Dynamic Stress and Cumulative Plastic Deformation of Calcareous Sand Filler Based on Shakedown Theory. JMSE 2023, 11, 195.
41. BS EN ISO 14688-2:2018 Geotechnical Investigation and Testing. Identification and Classification of Soil-Principles for a Classification; BS EN ISO 14688-2:2018; Under Review.; 2018; ISBN 978-0-580-87599-1.
42. Cai, Y.; Wu, T.; Guo, L.; Wang, J. Stiffness Degradation and Plastic Strain Accumulation of Clay under Cyclic Load with Principal Stress Rotation and Deviatoric Stress Variation. J. Geotech. Geoenviron. Eng. 2018, Vol. 144, 04018021.
43. Juneja, A.; Mohammed-Aslam, A.K. Post-Cyclic Undrained Response of Sand and Silt. Soil Dynamics and Earthquake Engineering 2020, Vol. 133, 106138.
44. Erken, A.; Can Ulker, B.M. Effect of Cyclic Loading on Monotonic Shear Strength of Fine-Grained Soils. Engineering Geology 2007, Vol. 89, pp. 243–257.